Axial Anomaly and Confinement in Two-dimensional QED:

Singular Behavior of Vacuum Polarization at Threshold

Bailing Ma and Chueng Ji

group meeting at NC State

Oct. 3, 2025

Outline

Introduction

- The Schwinger model, or QED(1+1), provides a useful tool in understanding the confinement mechanism of fermions.
- Because the gauge field lines are restricted to one dimension, the Schwinger model naturally provides a potential which confines fermions. When a fermion-antifermion pair is separated in 1+1D, it is energetically favorable to produce another fermion-antifermion pair out of the vacuum, shielding the originally separated fermion and antifermion not to yield any liberated fermion or anti-fermion.
- Such a mechanism of confinement (i.e. the "Schwinger mechanism") is tied to the intrinsic axial anomaly of the Dirac vacuum.

- Although the magnetic field is absent in 1+1D, the electric field can still be applied to the Dirac vacuum in 1+1D and excite a negative energy electron from the Dirac sea to a positive energy level.
- This pair creation of electron and positron can be regarded as the phenomenon of axial anomaly in quantum field theory.
- The level crossing phenomenon in 3+1D occurs essentially the same way as the electric field applies to the same direction of the magnetic field which sets the level density of the Dirac vacuum in 3+1D.

- While the axial anomaly in 3+1D is described by the triangle diagram amplitude proportional to the totally antisymmetric Levi-Civita symbol $\epsilon_{\mu\nu\alpha\beta}$, such an antisymmetric symbol cannot exist in 1+1D, however the axial anomaly in 1+1D can still be described by the two-point amplitude proportional to the lowest rank antisymmetric tensor $\epsilon_{\mu\nu}$.
- The axial anomaly amplitude $T_5^{\mu\nu}$ is related to the one-loop vacuum polarization amplitude $T^{\mu\nu}$, namely $T_5^{\mu\nu} = \epsilon^{\mu}_{\lambda} T^{\lambda\nu}$.

- The mass generation of the photon in 1+1D may be understood as modifying the free photon propagator by summing all the fermion loops in the propagation of the photon via the photon interaction with the Dirac vacuum.
- This mechanism of photon mass generation in 1+1D is distinct from the Higgs mechanism which provides the gauge boson mass by absorbing the Goldstone bosons in the 3+1D gauge field theory, as is well known in the electroweak unification of the Standard Model. In 1+1D, the spontaneous symmetry breaking cannot accompany the Goldstone boson according to Coleman's theorem.

To illustrate axial anomaly more heuristically in terms of the Dirac sea, one may consider the massless Schwinger model on a circle, with the fields satisfying the boundary conditions

$$A_\mu\left(t, x=-\frac{L}{2}\right)=A_\mu\left(t, x=\frac{L}{2}\right), \tag{1}$$

$$\psi\left(t, x=-\frac{L}{2}\right)=-\psi\left(t, x=\frac{L}{2}\right). \tag{2}$$

Since the Lagrangian is invariant under $U_V(1)$ and $U_A(1)$ symmetries, classically both the charge $Q(t)$ and axial-charge $Q^5(t)$ defined by

$$Q(t)=\int dx J_0(t,x) \tag{3}$$

and

$$Q^5(t)=\int dx J_0^5(t,x) \tag{4}$$

are conserved.

As $Q(t)$ and $Q^5(t)$ may be decomposed in terms of the left-moving and right-moving fermions, i.e.

$$Q(t) = Q_L(t) + Q_R(t) \tag{5}$$

and

$$Q^5(t) = Q_L(t) - Q_R(t), \tag{6}$$

the left-moving charge $Q_L(t)$ and the right-moving charge $Q_R(t)$ are separately conserved as well.

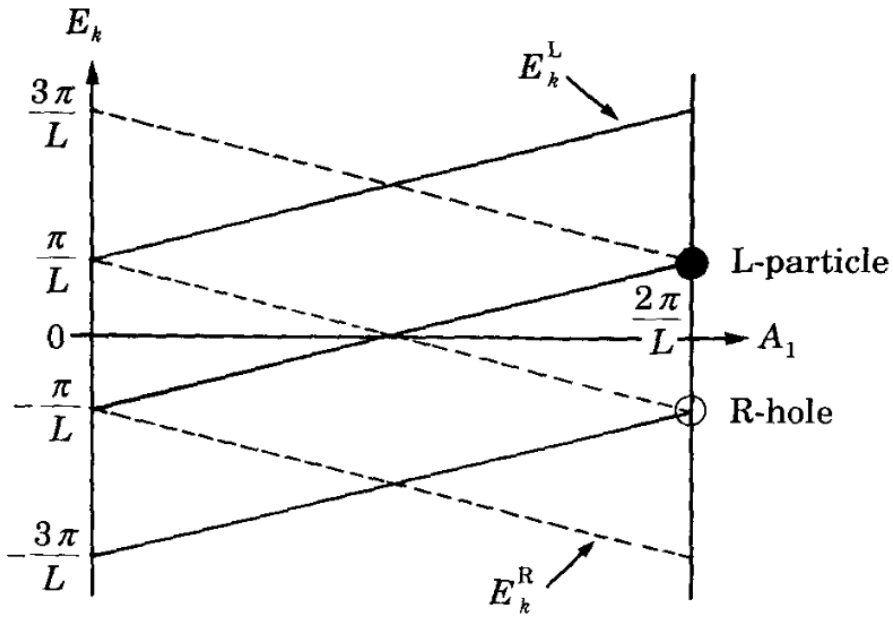

Crossing of the energy levels.

- However, this is no longer true in the quantum field theory due to the nature of the Dirac sea.
- Let us say the Dirac sea is provided by filling up all the negative energy levels and all the positive energy levels are empty at the zero gauge field, i.e. $A_1 = 0$.
- Now, applying an external electric field $\partial A_1(t, x)/\partial t$, one may increase A_1 from 0 to $2\pi/L$, creating a pair of L-particle and R-hole due to the response of both left-moving and right-moving fermions in the Dirac sea with respect to the applied external electric field.
- Such particle-hole pair creation under the external electric field may illustrate the axial anomaly in 1+1D. The charge is still conserved since the electric charge of the particle and the hole are opposite. The axial charges, however, are identical for both so that the total axial charge changes by 2 units.

Namely,

$$\Delta Q^5 = \frac{eL}{\pi}\Delta A_1 = \frac{eL}{\pi}\frac{2\pi}{L} = 2e, \tag{7}$$

and per time unit we have

$$\frac{\Delta Q^5}{\Delta t} = \frac{eL}{\pi}\frac{\Delta A_1}{\Delta t}. \tag{8}$$

Considering Eq. (4),

$$\frac{\partial}{\partial t}\int_0^L dx J_0^5(t,x) = \frac{e}{\pi}\frac{\partial}{\partial t}\int_0^L dx A_1(t). \tag{9}$$

We essentially obtained

$$\partial_0 J_0^5 = \frac{e}{\pi}\partial_0 A_1. \tag{10}$$

Or, written in a covariant way,

$$\partial^\mu J_\mu^5 = \frac{e}{\pi}\varepsilon_{\mu\nu}\partial^\mu A^\nu, \tag{11}$$

in contrast to the continuity equation of the vector current

$$\partial^\mu J_\mu = 0. \tag{12}$$

In 1+1D, one may surmise the relationship between the axial-vector current and the vector current given by

$$J^5_\mu = \varepsilon_{\mu\nu} J^\nu. \tag{13}$$

Realizing the off-diagonal element of the 1+1D field strength tensor $F^{\mu\nu}$ as the electric field $E(t, x)$, we may write

$$F^{\mu\nu} = \varepsilon^{\mu\nu} E, \tag{14}$$

where $F^{\mu\nu}$ satisfies the Maxwell's equation or the Gauss's law given by

$$\partial_\mu F^{\mu\nu} = e\bar{\psi}\gamma^\nu\psi = eJ^\nu. \tag{15}$$

From Eq. (11) as well as Eqs. (13)-(15), one can find the following equation

$$e\,\partial^\mu J^5_\mu = -\partial^\mu\partial_\mu E = \frac{e^2}{2\pi}\varepsilon_{\mu\nu}F^{\mu\nu} = -\frac{e^2}{\pi}E, \tag{16}$$

This derivation from the axial anomaly given by Eq. (11) provides the Klein-Gordon equation for the electric field $E(t, x)$ given by

$$\Box E = \frac{e^2}{\pi}E. \tag{17}$$

Main References

- D. G. Sutherland, Current algebra and the decay $\eta \to 3\pi$, Phys. Lett. 23 (1966) 384–385; D. G. Sutherland, Current algebra and some nonstrong mesonic decays, Nucl. Phys. B 2 (1967) 433–440
- N. K. Pak, P. Senjanovic, Axial Anomaly and Chiral Symmetry Breaking in Schwinger Model: A Canonical Approach, Phys. Lett. B 71 (1977) 333–336
- C. G. Callan, Jr., R. F. Dashen, D. J. Gross, The Structure of the Gauge Theory Vacuum, Phys. Lett. B 63 (1976) 334–340
- G. 't Hooft, Symmetry Breaking Through Bell-Jackiw Anomalies, Phys. Rev. Lett. 37 (1976) 8–11
- E. Katz, T. Okui, The 't Hooft model as a hologram, JHEP 01 (2009) 013. arXiv:0710.3402
- C. Adam, R. A. Bertlmann, P. Hofer, Overview on the anomaly and Schwinger term in two-dimensional QED, Riv. Nuovo Cim. 16N8 (1993) 1–52

Vacuum polarization and its dispersion relation

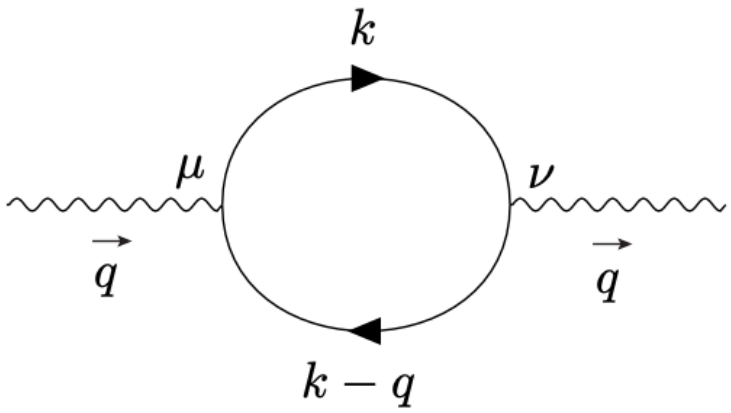

Figure: Feynman diagram for the photon self-energy at one-loop order.

As we said before, the axial anomaly in QED_2 is described by the two-point function as shown in the above figure. The amplitude with γ^μ and $\gamma^\nu\gamma_5$ instead of γ^μ and γ^ν can be related to the vacuum polarization by

$$T_5^{\mu\nu} = \varepsilon^{\nu\lambda} T_\lambda^\mu, \tag{18}$$

due to the relationship $\gamma^\mu\gamma^5 = \varepsilon^{\mu\nu}\gamma_\nu$ in $1+1$ dimensions.

For the discussion of the dispersion relation, we may briefly summarize the vacuum polarization amplitude

$$T^{\mu\nu}(q) = ie^2 \int \frac{d^2k}{(2\pi)^2} \frac{Tr\left[\gamma^\mu(\not{k}+m)\gamma^\nu(\not{k}-\not{q}+m)\right]}{\left[k^2-m^2+i\epsilon\right]\left[(k-q)^2-m^2+i\epsilon\right]}, \tag{19}$$

which is given by

$$\begin{aligned} & T^{\mu\nu}(q) \\ &= -\frac{e^2}{2\pi}\int_0^1 dx \frac{x(x-1)(2q^\mu q^\nu - g^{\mu\nu}q^2) + g^{\mu\nu}m^2}{x(x-1)q^2+m^2} + \frac{e^2}{2\pi}g^{\mu\nu}, \end{aligned} \tag{20}$$

using the Feynman parametrization. It manifestly satisfies the gauge invariance

$$q_\mu T^{\mu\nu}(q) = q_\nu T^{\mu\nu}(q) = 0. \tag{21}$$

Indeed, $T^{\mu\nu}(q)$ has the tensor structure of

$$T^{\mu\nu}(q) = T(q^2)\left(q^\mu q^\nu - g^{\mu\nu}q^2\right). \tag{22}$$

Using Eq. (18), one may write

$$T_5^{\mu\nu}(q) = T(q^2)\varepsilon^{\nu\lambda}\left(q^\mu q_\lambda - g_\lambda^\mu q^2\right), \tag{23}$$

fulfilling the vector current conservation,

$$q_\mu T_5^{\mu\nu}(q) = T(q^2)\varepsilon^{\nu\lambda} q_\mu \left(q^\mu q_\lambda - g_\lambda^\mu q^2\right) = 0, \tag{24}$$

as well as the anomalous axial vector current,

$$q_\nu T_5^{\mu\nu}(q) = T(q^2)\varepsilon^{\nu\lambda} q_\nu \left(q^\mu q_\lambda - g_\lambda^\mu q^2\right) = -q_\nu \varepsilon^{\nu\mu} q^2 T(q^2). \tag{25}$$

If one computes the two-point function with a vector and a pseudo-scalar current,

$$P_5^\mu(q) = ie^2 \int \frac{d^2k}{(2\pi)^2} \frac{Tr\left[\gamma^\mu(\not{k}+m)\gamma_5(\not{k}-\not{q}+m)\right]}{\left[k^2-m^2+i\epsilon\right]\left[(k-q)^2-m^2+i\epsilon\right]}, \tag{26}$$

one gets

$$P_5^\mu(q) = \frac{e^2 m}{2\pi} \int_0^1 dx \frac{\varepsilon^{\mu\nu} q_\nu}{x(x-1)q^2+m^2}. \tag{27}$$

Thus, one can write

$$q_\nu T_5^{\mu\nu}(q) = 2mP_5^\mu(q) + \frac{e^2}{\pi} q_\lambda \varepsilon^{\lambda\mu}. \tag{28}$$

This is the famous axial anomaly which reduces to

$$q_\nu T_5^{\mu\nu}(q) = \frac{e^2}{\pi} q_\nu \varepsilon^{\nu\mu} \tag{29}$$

in the massless case.

After the integration of the Feynman parameter x, the explicit form of the $T(q^2)$ function in $1+1$ dimensions is given by

$$T(q^2) = -\frac{e^2}{\pi q^2}\left[1 - \frac{m^2/q^2}{\sqrt{1/4 - m^2/q^2}} \ln\left(\frac{1 - \frac{1}{2\sqrt{1/4-m^2/q^2}}}{1 + \frac{1}{2\sqrt{1/4-m^2/q^2}}}\right)\right]. \quad (30)$$

- The process of a pair creation of fermion and anti-fermion can occur above the threshold, $q^2 > 4m^2$, while no such process can be allowed below the threshold, $q^2 < 4m^2$.
- Interestingly, $T(q^2)$ diverges at exactly $q^2 = 4m^2$.
- We interpret this singular behavior at $q^2 = 4m^2$ as the symptom of the confinement in QED(1+1), namely a fermion or anti-fermion cannot be on its mass shell, á la "Schwinger mechanism".

We may contrast this singular behavior of the vacuum polarization amplitude in 1+1D with the 3+1D vacuum polarization amplitude $T_{3+1}(q^2)$ given by

$$\begin{aligned} & T_{3+1}(q^2) \\ =& -\frac{\alpha}{3\pi}\left[\log\frac{\Lambda_{PV}^2}{m^2} - 6\int_0^1 dx\, x(1-x)\log\left(1-\frac{q^2}{m^2}x(1-x)\right)\right], \end{aligned} \tag{31}$$

where Λ_{PV} is the Paul-Villar's regularization parameter for the regularization of UV-divergence in 3+1D. The regularization scale independent formula may also be defined as

$$\begin{aligned} & \hat{T}_{3+1}(q^2) \equiv T_{3+1}(q^2) - T_{3+1}(0) \\ =& \frac{2\alpha}{\pi}\int_0^1 dx\, x(1-x)\log\left(\frac{m^2}{m^2 - x(1-x)q^2}\right). \end{aligned} \tag{32}$$

We verify that both $T(q^2)$ in 1+1D and $\hat{T}_{3+1}(q^2)$ satisfy the dispersion relation (DR), respectively. In 1+1D, $T(q^2)$ satisfies the DR given by

$$\begin{aligned}
\mathrm{Re}\, T(q^2) &= \frac{1}{\pi} P \int_{-\infty}^{+\infty} \frac{\mathrm{Im}\, T(q'^2)}{q'^2 - q^2} dq'^2, \\
\mathrm{Im}\, T(q^2) &= -\frac{1}{\pi} P \int_{-\infty}^{+\infty} \frac{\mathrm{Re}\, T(q'^2)}{q'^2 - q^2} dq'^2,
\end{aligned} \tag{33}$$

where P indicates the Cauchy principal value. In 3+1D, $\hat{T}_{3+1}(q^2)$ satisfies the subtracted DR given by

$$\begin{aligned}
\mathrm{Re}\, \hat{T}_{3+1}(q^2) &= \frac{1}{\pi} \left(P \int_{-\infty}^{+\infty} \frac{\mathrm{Im}\, \hat{T}_{3+1}(q'^2)}{q'^2 - q^2} dq'^2 - P \int_{-\infty}^{+\infty} \frac{\mathrm{Im}\, \hat{T}_{3+1}(q'^2)}{q'^2 - q_0^2} dq'^2 \right) \\
&= \frac{q^2 - q_0^2}{\pi} P \int_{-\infty}^{+\infty} \frac{\mathrm{Im}\, \hat{T}_{3+1}(q'^2)}{(q'^2 - q^2)(q'^2 - q_0^2)} dq'^2, \\
\mathrm{Im}\, \hat{T}_{3+1}(q^2) &= -\frac{1}{\pi} \left(P \int_{-\infty}^{+\infty} \frac{\mathrm{Re}\, \hat{T}_{3+1}(q'^2)}{q'^2 - q^2} dq'^2 - P \int_{-\infty}^{+\infty} \frac{\mathrm{Re}\, \hat{T}_{3+1}(q'^2)}{q'^2 - q_0^2} dq'^2 \right) \\
&= -\frac{q^2 - q_0^2}{\pi} P \int_{-\infty}^{+\infty} \frac{\mathrm{Re}\, \hat{T}_{3+1}(q'^2)}{(q'^2 - q^2)(q'^2 - q_0^2)} dq'^2,
\end{aligned} \tag{34}$$

where q_0^2 is taken to be 0 to cross the origin at $q^2 = 0$ in agreement with Eq. (32).

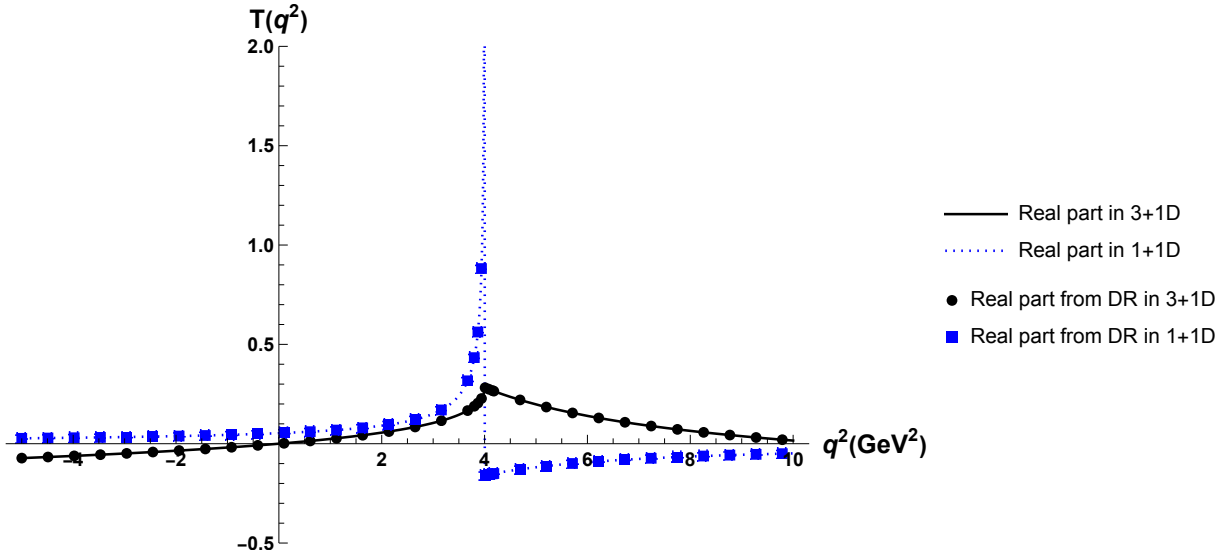
T(q^2)
2.0
1.5
1.0
0.5
−0.5
−4
−2
2
4
6
8
10
q^2(GeV^2)
Real part in 3+1D
Real part in 1+1D
Real part from DR in 3+1D
Real part from DR in 1+1D

(a)

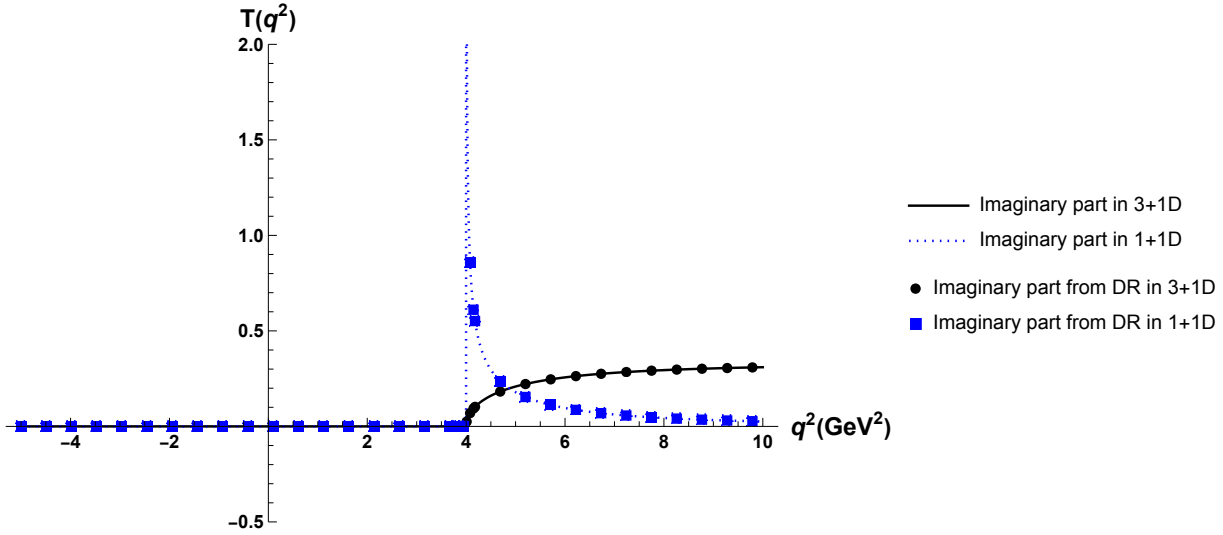
T(q^2)
2.0
1.5
1.0
0.5
−0.5
−4
−2
2
4
6
8
10
q^2(GeV^2)
Imaginary part in 3+1D
Imaginary part in 1+1D
Imaginary part from DR in 3+1D
Imaginary part from DR in 1+1D

(b)

- Plot: the real and imaginary parts of $T(q^2)$ in both 1+1D and 3+1D, where the data points represent the DR result while the lines represent the direct result.
- In both cases the (unsubtracted or subtracted) DR is satisfied, even though in 1+1D case both the real and imaginary parts diverge at $q^2 = 4m^2$.
- No physical pair production of on-mass-shell particle and anti-particle at the $q^2 = 4m^2$ threshold in the 1+1D case, although virtual off-mass-shell particle and anti-particle pair productions may occur within the quantum mechanical uncertainty.
- 3+1D: Both functions of $\mathrm{Re}[T(q^2)]$ and $\mathrm{Im}[T(q^2)]$ are connected at $q^2 = 4m^2$ and finite for the entire time-like region above the threshold. As q^2 gets larger, $\mathrm{Re}[T(q^2)]$ grows in its value while $\mathrm{Im}[T(q^2)]$ saturates to a finite value.
- 1+1D: A jump in value, for $\mathrm{Re}[T(q^2)]$ from $+\infty$ to $-\frac{1}{2\pi}$, and for $\mathrm{Im}[T(q^2)]$ from 0 to $+\infty$. Both $\mathrm{Re}[T(q^2)]$ and $\mathrm{Im}[T(q^2)]$ die out to zero as q^2 gets larger.

Photon mass generation in 1+1D

- The photon mass generation in 1+1D may be understood from the interaction of the propagating photon with the Dirac vacuum which leads to the photon self-energy amplitude as shown before.
- The geometric sum of photon self-energy process may lead to the photon mass gap amplitude shown below.
- We note that the geometrical sum of the one-loop $T(q^2)$, i.e. $\frac{1}{1+T(q^2)}$, removes the singularity at $q^2 = 4m^2$. The photon mass can also be immediately seen in the result of the geometric sum.

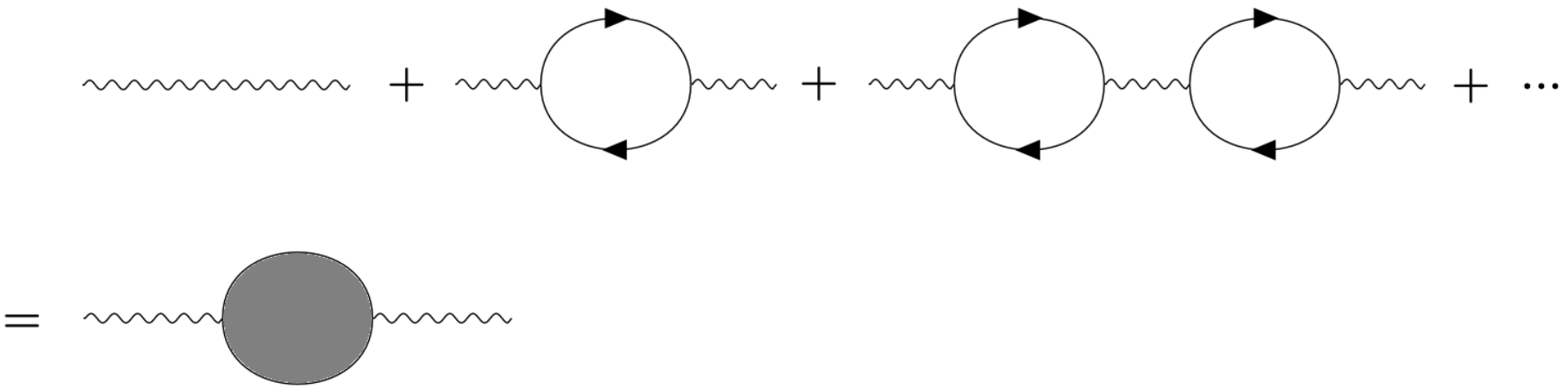

Figure: Mass gap equation for the photon in QED_{1+1}.

Bare photon propagator:

$$\left(g_{\mu\nu} - \frac{q_\mu q_\nu}{q^2}\right) D_0(q^2) \tag{35}$$

where

$$D_0(q^2) = -\frac{1}{q^2 + i\epsilon}. \tag{36}$$

Dressed photon propagator:

$$D_{\mu\nu}(q) = \left(g_{\mu\nu} - \frac{q_\mu q_\nu}{q^2}\right) D(q^2), \tag{37}$$

where

$$D(q^2) = -\frac{1}{q^2 + q^2\, T(q^2)}. \tag{38}$$

This result is obtained from the geometrical sum

$$
\begin{aligned}
& i\left(g_{\mu\nu}-\frac{q_\mu q_\nu}{q^2}\right) D_0(q^2) \\
& + i\left(g_{\mu\nu}-\frac{q_\mu q_\nu}{q^2}\right) D_0(q^2)\; iT^{\mu\nu}(q^2)\; i\left(g_{\mu\nu}-\frac{q_\mu q_\nu}{q^2}\right) D_0(q^2) \\
& + i\left(g_{\mu\nu}-\frac{q_\mu q_\nu}{q^2}\right) D_0(q^2)\; iT^{\mu\nu}(q^2)\; i\left(g_{\mu\nu}-\frac{q_\mu q_\nu}{q^2}\right) D_0(q^2) \\
& \cdot iT^{\mu\nu}(q^2)\; i\left(g_{\mu\nu}-\frac{q_\mu q_\nu}{q^2}\right) D_0(q^2) + \ldots \\
= & \; i\left(g_{\mu\nu}-\frac{q_\mu q_\nu}{q^2}\right) D(q^2). \qquad (39)
\end{aligned}
$$

In the case of massless fermions ($m = 0$), we use Eq. (30) to obtain

$$
D_{\mu\nu}(q) = -\frac{g_{\mu\nu} - q_\mu q_\nu/q^2}{q^2 - e^2/\pi + i\epsilon}. \qquad (40)
$$

This provides the photon propagator with mass $m_\gamma = e/\sqrt{\pi}$. Moreover, the geometric sum shown in the dressed photon figure eliminates the singularity of the vacuum polarization amplitude $T(q^2)$ at $q^2 = 4m^2$. As

$$D(q^2) = \frac{1}{1 + T(q^2)} D_0(q^2), \tag{41}$$

we can see in the plot of plot of $\frac{1}{1+T(q^2)}$ that both the real and imaginary parts of $\frac{1}{1+T(q^2)}$ are finite everywhere, and also they satisfy the dispersion relation (DR).

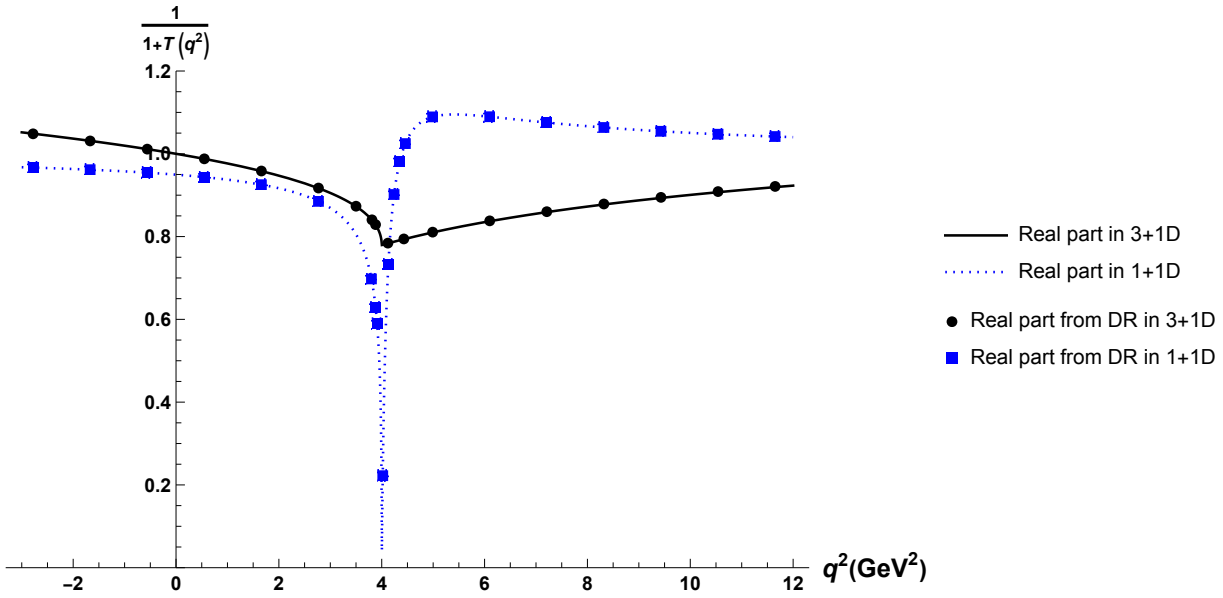
$\frac{1}{1+T(q^2)}$
1.2
1.0
0.8
0.6
0.4
0.2
−2
0
2
4
6
8
10
12
$q^2(\mathrm{GeV}^2)$
Real part in 3+1D
Real part in 1+1D
Real part from DR in 3+1D
Real part from DR in 1+1D

(a)

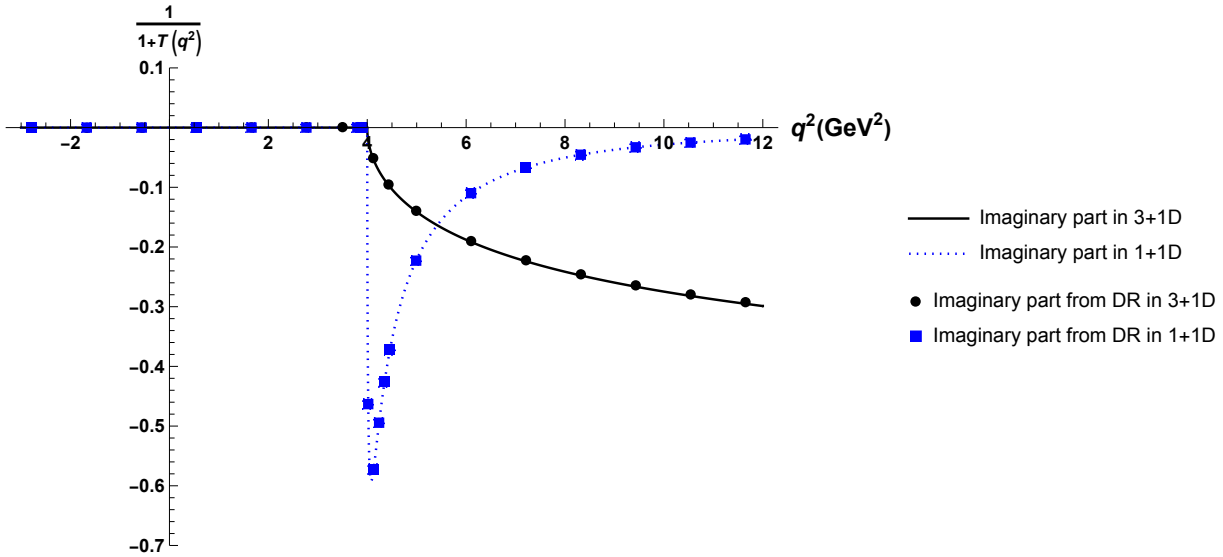
$\frac{1}{1+T(q^2)}$
0.1
−0.1
−0.2
−0.3
−0.4
−0.5
−0.6
−0.7
−2
2
4
6
8
10
12
$q^2(\mathrm{GeV}^2)$
Imaginary part in 3+1D
Imaginary part in 1+1D
Imaginary part from DR in 3+1D
Imaginary part from DR in 1+1D

(b)

Physical observables: cross section and R-ratio

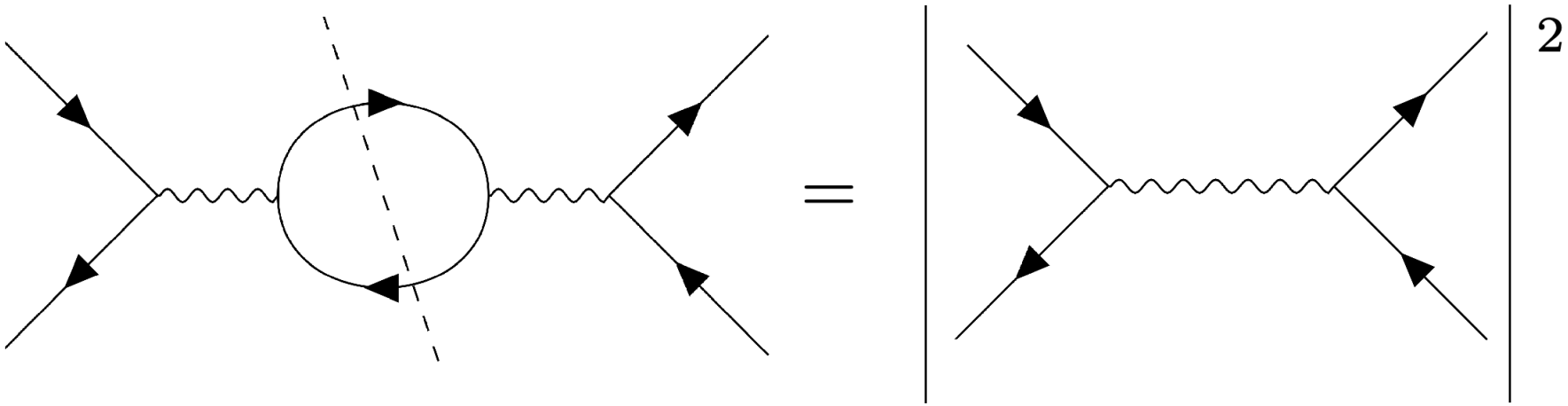

Figure: Total cross-section of $e^+e^- \to \mu^+\mu^-$.

In $3+1$ dimensions, the scattering cross section of the $e^+e^- \to \mu^+\mu^-$ process is an exemplary physical observable. In the leading order of the QED coupling constant, the total unpolarized cross section of $e^+e^- \to \mu^+\mu^-$ (See Fig. 3) is given by

$$\begin{aligned}
&\sigma_{\text{tot},3+1}^{e^+e^-\to\mu^+\mu^-} \\
=&\frac{1}{2w_e}\frac{1}{(2\pi)^2}\int\frac{d^3p_1'}{2p_1'^0}\int\frac{d^3p_2'}{2p_2'^0}\delta^{(4)}(p_1+p_2-p_1'-p_2')\,|\overline{\mathcal{M}}_{3+1}|^2, \qquad (42)
\end{aligned}$$

where $w_e \equiv q^2\sqrt{1-\frac{4m_e^2}{q^2}}$ and

$$\begin{aligned}
|\overline{\mathcal{M}}_{3+1}|^2 = \frac{8e^4}{q^4}\,&(p_1\cdot p_1'\;p_2\cdot p_2' + p_1\cdot p_2'\;p_2\cdot p_1' + p_1\cdot p_2 m_\mu^2 \\
&+p_1'\cdot p_2' m_e^2 + 2m_e^2 m_\mu^2)\,, \qquad (43)
\end{aligned}$$

using the photon propagator $D_0(q^2) = -\frac{1}{q^2+i\varepsilon}$. Using the phase space integration $\int\frac{d^3p_2'}{2p_2'^0} = \int d^4p_2'\delta\left(p_2'^2 - m_\mu^2\right)$, and taking the center-of-mass frame, i.e., $p_1'^0 = p_2'^0 = \frac{\sqrt{q^2}}{2} = \frac{\sqrt{s}}{2}$, one can find

$$\sigma^{e^+e^-\to\mu^+\mu^-}_{\text{tot},3+1}$$

$$=\frac{1}{2w_e}\frac{1}{(2\pi)^2}\int dp_1'^0\frac{\sqrt{(p_1'^0)^2-m_\mu^2}}{2}\frac{1}{2q^0}\delta(p_1'^0-\frac{q^2}{2q^0})d\Omega\ |\overline{\mathcal{M}}_{3+1}|^2. \quad (44)$$

One can obtain

$$\sigma^{e^+e^-\to\mu^+\mu^-}_{\text{tot},3+1}=\frac{1}{64\pi^2 s}\frac{\sqrt{1-\frac{4m_\mu^2}{q^2}}}{\sqrt{1-\frac{4m_e^2}{q^2}}}\int d\Omega\ |\overline{\mathcal{M}}_{3+1}|^2\Theta(q^2-4m_\mu^2), \quad (45)$$

where the Heaviside theta function is to ensure that $q^2 > 4m_\mu^2$. Because $m_\mu > m_e$, this automatically ensures $q^2 > 4m_e^2$ also.

In contrast, the result in 1+1D corresponding to Eqs. (42)-(43) is given by

$$\sigma_{\text{tot},1+1}^{e^+e^-\to\mu^+\mu^-} = \frac{1}{2w_e}\int\frac{dp_1'^1}{2p_1'^0}\int\frac{dp_2'^1}{2p_2'^0}\delta^{(2)}(p_1+p_2-p_1'-p_2')\,|\overline{\mathcal{M}}_{1+1}|^2, \tag{46}$$

where

$$|\overline{\mathcal{M}}_{1+1}|^2 = \frac{2e^4}{q^4}(p_1\cdot p_1'\ p_2\cdot p_2' + p_1\cdot p_2'\ p_2\cdot p_1' - p_1\cdot p_2\ p_1'\cdot p_2' + m_e^2 m_\mu^2). \tag{47}$$

The integration of the momentum variables p_1' and p_2' of Eq.(46) can be done straightforwardly using the formulae

$$I_2 = \int\frac{dp_1'^1}{2p_1'^0}\int\frac{dp_2'^1}{2p_2'^0}\delta^{(2)}(q-p_1'-p_2')f(p_1'\cdot p_2') = \frac{1}{w_\mu}f\left(\frac{1}{2}(q^2-2m_\mu^2)\right), \tag{48}$$

$$I_2^{\mu\nu} = \int\frac{dp_1'^1}{2p_1'^0}\int\frac{dp_2'^1}{2p_2'^0}\delta^{(2)}(q-p_1'-p_2')f(p_1'\cdot p_2')p_1'^\mu p_2'^\nu = \left[\left(\frac{q^2}{4}-m_\mu^2\right)g^{\mu\nu}+\frac{m_\mu^2}{q^2}q^\mu q^\nu\right]I_2, \tag{49}$$

where

$$w_\mu \equiv q^2 \sqrt{1 - \frac{4m_\mu^2}{q^2}}. \tag{50}$$

Taking $f(p_1' \cdot p_2') = \frac{1}{2w_e} \frac{2e^4}{q^4} \left(-p_1 \cdot p_2 \; p_1' \cdot p_2' + m_e^2 m_\mu^2\right)$ for Eq. (48) and $f(p_1' \cdot p_2') = 1$ along with the external tensor $\frac{1}{2w_e} \frac{2e^4}{q^4} \left(p_{1\mu} p_{2\nu} + p_{2\mu} p_{1\nu}\right)$ outside the integration of the p_1' and p_2' variables for Eq. (49), and noting that

$$p_1' \cdot p_2' = \frac{q^2 - 2m_\mu^2}{2}, \tag{51}$$

$$p_1 \cdot p_2 = \frac{q^2 - 2m_e^2}{2}, \tag{52}$$

and

$$p_1' \cdot q = p_2' \cdot q = p_1 \cdot q = p_2 \cdot q = \frac{q^2}{2}, \tag{53}$$

we obtain

$$\sigma_{\text{tot},1+1}^{e^+e^-\to\mu^+\mu^-} = \frac{2e^4 m_e^2 m_\mu^2}{q^8} \frac{1}{\sqrt{1-\frac{4m_e^2}{q^2}}\sqrt{1-\frac{4m_\mu^2}{q^2}}} \Theta(q^2-4m_\mu^2). \tag{54}$$

However, this cross-section in 1+1D is apparently divergent when q^2 approaches the threshold of the $\mu^+\mu^-$ pair production, $q^2 = 4m_\mu^2$. Due to the two missing dimensions in contrast to the 3+1 dimensions, the factor $\sqrt{1-\frac{4m_\mu^2}{q^2}}$ here is positioned on the denominator rather than the numerator. This corresponds to the singular behavior of the vacuum polarization function $T(q^2)$ at $q^2 = 4m^2$ as we noticed earlier. We have interpreted the singular behavior at $q^2 = 4m^2$ as the symptom of the confinement in QED(1+1), namely a fermion or anti-fermion cannot be on its mass shell, á la "Schwinger mechanism".

However, the singularity of the vacuum polarization amplitude $T(q^2)$ at $q^2 = 4m^2$ is removed in the geometric sum to yield the dressed photon propagator given by Eq. (38). Replacing the bare photon propagator by the dressed photon propagator, we get

$$\sigma_{\text{tot},1+1}^{e^+e^-\to\mu^+\mu^-} = \frac{2e^4 m_e^2 m_\mu^2}{\left|q^2 + q^2 T_{\mu^+\mu^-}(q^2)\right|^2} \frac{1}{q^4} \frac{1}{\sqrt{1-\frac{4m_e^2}{q^2}}} \frac{1}{\sqrt{1-\frac{4m_\mu^2}{q^2}}} \Theta(q^2 - 4m_\mu^2). \tag{55}$$

Now, plugging in the self-energy of the photon dressed by muon loops, $T_{\mu^+\mu^-}(q^2)$, i.e. $T(q^2)$ with $m = m_\mu$, we have

$$\sigma_{\text{tot},1+1}^{e^+e^-\to\mu^+\mu^-} = \frac{2e^4 m_e^2 m_\mu^2}{\left|q^2 - \frac{e^2}{\pi}\left[1 - \frac{m_\mu^2/q^2}{\sqrt{1/4 - m_\mu^2/q^2}} \ln\left(\frac{1 - \frac{1}{2\sqrt{1/4-m_\mu^2/q^2}}}{1 + \frac{1}{2\sqrt{1/4-m_\mu^2/q^2}}}\right)\right]\right|^2} \frac{1}{q^4} \frac{1}{\sqrt{1-\frac{4m_e^2}{q^2}}} \frac{1}{\sqrt{1-\frac{4m_\mu^2}{q^2}}} \Theta(q^2 - 4m_\mu^2) \tag{56}$$

which is no longer divergent at $q^2 = 4m_\mu^2$ due to the loop corrections.

Taking $e = 1$ and $m_e = m_\mu = 1$ as an example, we show the plot of $\sigma_{\text{tot},1+1}^{e^+e^-\to\mu^+\mu^-}(q^2)$ below, where we can see the different behavior of Eqs. (54) and (56) near $q^2 = 4$ in that one diverges and the other does not.

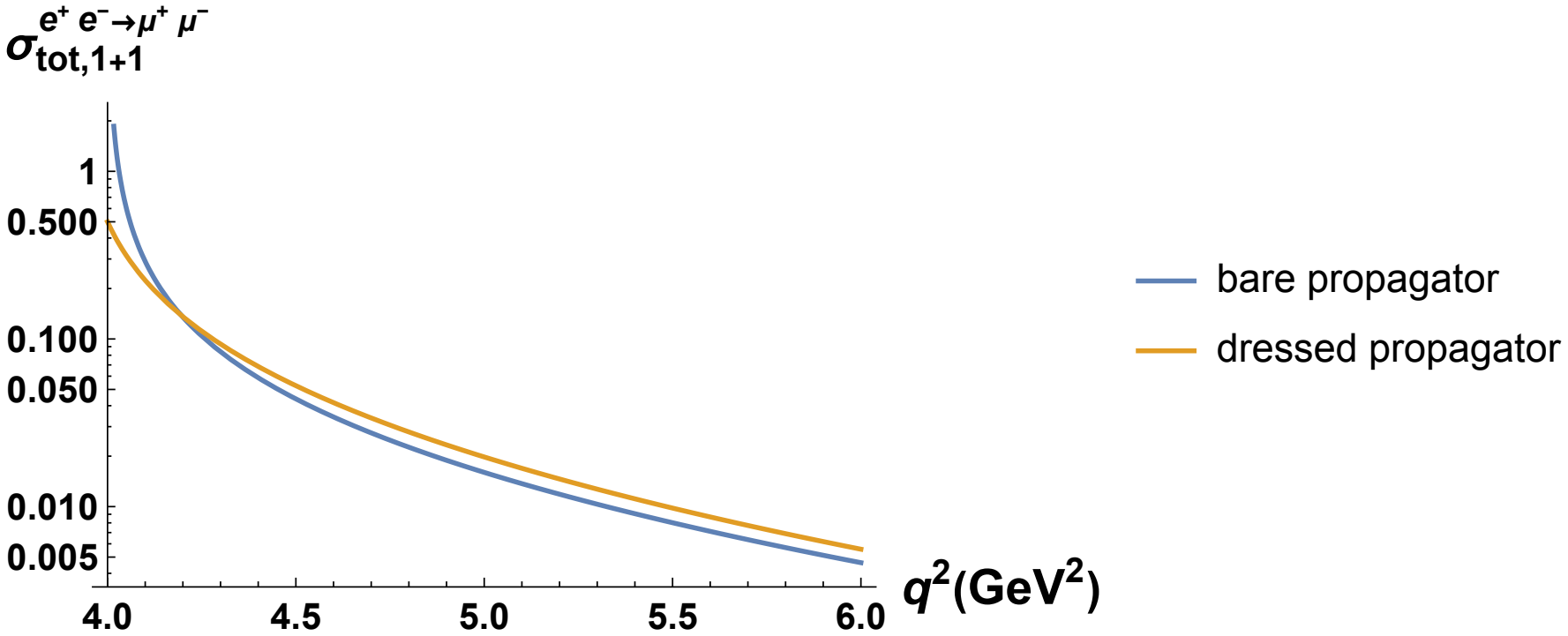

Figure: Total cross-section of $e^+e^- \to \mu^+\mu^-$ in 1+1D plotted as a function of q^2, using the bare propagator and the dressed propagator of the photon, respectively.

Having computed the total cross section of the fermion and anti-fermion pair production from the e^+e^- annihilation process, we may now discuss the ratio of the total cross sections between the quarks and the leptons known as the R ratio in 3+1D given by

$$R_{3+1} = \frac{\sigma_{\text{tot},3+1}^{e^+e^-\to q\bar{q}}}{\sigma_{\text{tot},3+1}^{e^+e^-\to \mu^+\mu^-}}. \tag{57}$$

Typically in the R ratio, the quark masses are not neglected while the lepton masses are neglected for the discussion of the different quark flavor thresholds which have been measured from the experiments.
For the lepton pair production cross section, neglecting both the electron and muon masses, we get the spin-averaged invariant amplitude square given by

$$|\overline{\mathcal{M}}_{3+1}|^2 \longrightarrow 2e^4 \frac{t^2+u^2}{s^2}, \tag{58}$$

where s, t and u are the usual Mandelstam variables.

Noting that in the ultra-relativistic limit

$$-\frac{u}{s} \longrightarrow \frac{1}{2}(1+\cos\theta) \tag{59}$$

$$-\frac{t}{s} \longrightarrow \frac{1}{2}(1-\cos\theta), \tag{60}$$

one can get

$$\sigma^{e^+e^-\to\mu^+\mu^-}_{\text{tot},3+1} = \frac{\alpha^2}{4\pi^2 s}\int d\Omega \ \left(1+\cos^2\theta\right), \tag{61}$$

where $\alpha = \frac{e^2}{4\pi}$. Integrating over the solid angle gives the familiar result

$$\sigma^{e^+e^-\to\mu^+\mu^-}_{\text{tot},3+1} = \frac{4\pi\alpha^2}{3s}. \tag{62}$$

Similarly, the numerator of Eq. (57) can be obtained by replacing the muon mass in the derivation of Eqs. (42) through (45) with the quark masses m_{q_i} and noting that the quark charges Q_{q_i} are different from the electron and muon charge e. Using

$$p_1 \cdot p_1' = p_2 \cdot p_2' = \frac{m_{q_i}^2 - t}{2} \tag{63}$$

$$p_1 \cdot p_2' = p_2 \cdot p_1' = \frac{m_{q_i}^2 - u}{2} \tag{64}$$

as well as Eq. (52) and Eqs. (59)-(60), we obtain

$$\sigma_{\text{tot},3+1}^{e^+e^- \to q\bar{q}}$$

$$= \sum_{q_i} \frac{1}{4\pi s} \sqrt{1 - \frac{4m_{q_i}^2}{s}} Q_{q_i}^2 e^2 \left(\frac{1}{3} + \frac{m_{q_i}^4}{s^2} + 2\frac{m_{q_i}^2}{s} \right) \Theta(q^2 - 4m_{q_i}^2). \tag{65}$$

The R ratio in Eq. (57) is then given by

$$R_{3+1} = 3\sum_{q_i}\sqrt{1-\frac{4m_{q_i}^2}{q^2}}\frac{Q_{q_i}^2}{e^2}\left(1+3\frac{m_{q_i}^4}{s^2}+6\frac{m_{q_i}^2}{s}\right)\Theta(q^2-4m_{q_i}^2), \quad (66)$$

where the color factor 3 is taken into account.
The analogous R ratio in $1+1$ dimensions can then be computed from the cross section of $e^+e^- \to q_i\bar{q}_i$ for each quark flavor q_i to that of $e^+e^- \to \mu^+\mu^-$ and sum them over all the quark flavors. In contrast to the cross sections in 3+1D, we need to take into account the overall mass factors appearing in Eq. (56). In the limit of both $m_e \to 0$ and $m_\mu \to 0$, the total cross section $\sigma_{\rm tot}^{e^+e^-\to\mu^+\mu^-}$ scaled by m_e and m_μ in 1+1D can be obtained from Eq. (56) as

$$\frac{\sigma_{\rm tot,1+1}^{e^+e^-\to\mu^+\mu^-}}{m_e^2 m_\mu^2} = \frac{2e^4}{q^4\left(q^2-\frac{e^2}{\pi}\right)^2}\Theta(q^2). \quad (67)$$

Similarly, we may scale the individual total cross section for each quark flavor q_i denoted by $\sigma_{\text{tot},1+1}^{e^+e^-\to q_i\bar{q}_i}$ by m_e and m_{q_i} replacing m_μ by m_{q_i} in Eq. (56) and obtain

$$\frac{\sigma_{\text{tot},1+1}^{e^+e^-\to q_i\bar{q}_i}}{m_e^2 m_{q_i}^2} = \frac{2Q_{q_i}^2 e^2}{\left| q^2 - \frac{Q_{q_i}^2}{\pi}\left[1 - \frac{m_{q_i}^2/q^2}{\sqrt{1/4 - m_{q_i}^2/q^2}} \ln\left(\frac{1 - \frac{1}{2\sqrt{1/4 - m_{q_i}^2/q^2}}}{1 + \frac{1}{2\sqrt{1/4 - m_{q_i}^2/q^2}}}\right)\right]\right|^2} \cdot \frac{1}{q^4} \frac{1}{\sqrt{1 - \frac{4m_e^2}{q^2}}} \frac{1}{\sqrt{1 - \frac{4m_{q_i}^2}{q^2}}} \Theta(q^2 - 4m_{q_i}^2), \tag{68}$$

where we did not neglect any mass although we will take practically $m_e = 0$ in our numerical computations.

Summing over the quark flavors in Eq. (68) and taking its ratio to Eq. (67), we may define the R ratio in 1+1D as

$$R_{1+1} = \frac{3\sum_{q_i} \frac{\sigma^{e^+e^-\to q_i\bar{q}_i}_{\text{tot},1+1}}{m_e^2 m_{q_i}^2}}{\frac{\sigma^{e^+e^-\to \mu^+\mu^-}_{\text{tot},1+1}}{m_e^2 m_\mu^2}}, \tag{69}$$

where the color factor 3 is taken into account.
To contrast the behaviors of R_{1+1} and R_{3+1} near the thresholds of different quark flavors, we plot them below taking $e = 1$, the masses of the heavier quarks as $m_s = 0.5$ GeV, $m_c = 1.5$ GeV, and $m_b = 5$ GeV and ignoring the u, d quark as well as the electron and muon masses. While we can clearly see the thresholds at 1, 9, and 100 GeV^2, which are the $4m_s^2$, $4m_c^2$, and $4m_b^2$, respectively, we note that the two R ratios have quite different behavior near these thresholds.

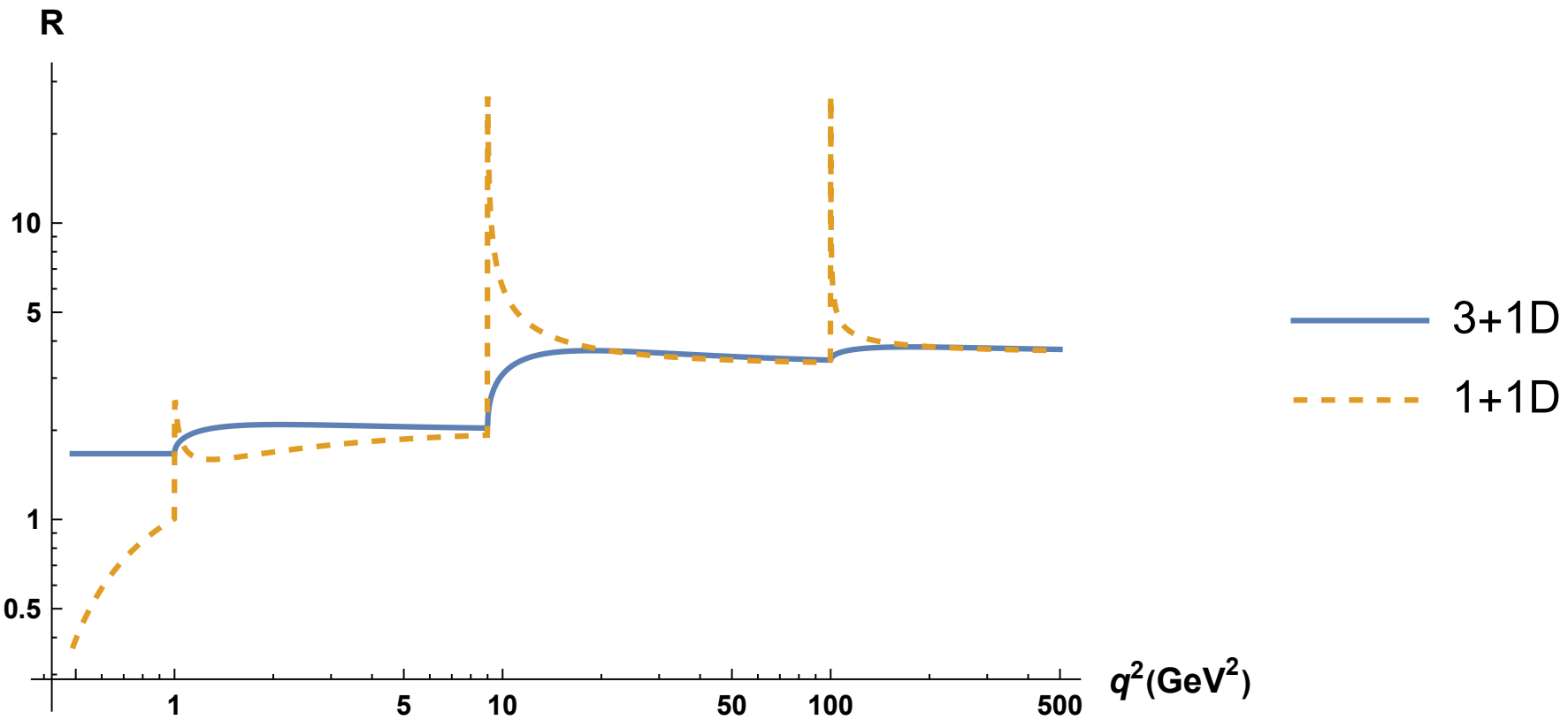

Figure: The R ratio in 1+1D and 3+1D plotted as a function of q^2.

Conclusions and outlook

- In this work, we studied the QED vacuum polarizations of 1+1D vs. 3+1D to investigate the nature of threshold singularity.
- We found that our results both in 1+1D and 3+1D satisfy the dispersion relation (DR), respectively, assuring their validity supported by the first principle quantum field theory.
- We note that the 1+1D QED vacuum polarization exhibits the fermion threshold singularity at the one-loop level, which may be interpreted as the symptom of the fermion confinement in 1+1D, namely no isolated fermion can be found in 1+1D, *'a la* Schwinger mechanism.
- While the geometric sum of the one-loop vacuum polarization amplitudes regulates the divergence appearing in the single loop amplitude, the regularized result comes with the mass generation of the gauge field. When the photon gets massive in 1+1D QED, it acquires the longitudinal polarization as there are no transverse polarizations of the photon in 1+1D.

- This indicates the correlation between the charge confinement and the photon mass generation in 1+1D. Thus, in 1+1D, the charge confinement and the chiral symmetry breaking appear tied together with the photon mass generation.
- This is quite remarkable from the QCD perspectives, as the color confinement and chiral symmetry breaking are still regarded as two distinguished and separate phenomena.
- More in-depth studies are needed on the underpinning mechanism to understand both the charge confinement and the chiral symmetry breaking together within the common relativistic quantum field theoretic framework.
- Further studies on the time-ordered processes of the fermion and anti-fermion pair creation and annihilation are underway contrasting the two distinguished forms of relativistic dynamics proposed by Dirac, namely the instant form dynamics and the light-front dynamics.

Thank you for your attention! [1]

[1] Paper in preprint: arXiv:2510.17074